

## THE VARIABILITY OF THE Hg II $\lambda$ 3984 LINE OF THE MERCURY-MANGANESE STAR $\alpha$ ANDROMEDAE

SAUL J. ADELMAN<sup>1</sup>

Department of Physics, The Citadel, 171 Moultrie Street, Charleston, SC 29409; adelmans@citadel.edu

AUSTIN F. GULLIVER<sup>1</sup>

Department of Physics and Astronomy, Brandon University, Brandon, MB R7A 6A9, Canada; gulliver@brandonu.ca

OLEG P. KOCHUKHOV

Uppsala Astronomical Observatory, Box 515, SE751-20, Uppsala, Sweden; oleg@astro.uu.se

AND

TANYA A. RYABCHIKOVA

Institute of Astronomy, Russian Academy of Sciences, 48 Pyatnitskaya Street, 109017 Moscow, Russia; and Institute for Astronomy, University of Vienna, Türkenschanzstrasse 17, A-1180 Vienna, Austria; ryabchik@antonio.inasan.rssi.ru, ryabchik@tycho.univie.ac.at

Received 2002 January 4; accepted 2002 April 10

### ABSTRACT

The variability of the Hg II  $\lambda$ 3984 line in the primary of the binary star  $\alpha$  And was discovered through the examination of high-dispersion spectra with signal-to-noise ratios greater than 500. This first definitively identified spectrum variation in any mercury-manganese star is not due to the orbital motion of the companion. Rather, the variation is produced by the combination of the 2.38236 day period of rotation of the primary that we determined and a nonuniform surface distribution of mercury that is concentrated in its equatorial region. If the surface mercury distribution exhibits long-term stability, then it is likely that a weak magnetic field operates in its atmosphere, but if changes are observed in the line profile over a period of a few years, then these would constitute direct evidence for diffusion.

*Subject headings:* binaries: general — binaries: spectroscopic — stars: chemically peculiar — stars: individual ( $\alpha$  Andromedae)

### 1. INTRODUCTION

The mercury-manganese (HgMn) stars populate the main-sequence band between 10,500 and 15,000 K. They exhibit a remarkable variety of abundance anomalies with both depletions (e.g., N; Roby, Leckrone, & Adelman 1999) and enhancements (e.g., Hg, which can also include anomalous isotopic mixtures; Leckrone, Wahlgren, & Johansson 1991; Wahlgren et al. 1995), which are thought to be produced in an extremely hydrodynamically stable environment from the separation of elements by radiatively driven diffusion and gravitational settling (Michaud 1970). Seaton (1996, 1999) used Opacity Project data in calculations that suggest that the manganese-rich atmospheres of these stars are a very slowly changing time-variable surface, the result of radiatively driven diffusion that occurs deep in the stellar envelope.

A few published papers suggest that certain HgMn stars might be variable on timescales of a day or a few days. Because of its higher signal-to-noise ratio (S/N), the photometric evidence has been considered to be more plausible than the spectroscopic evidence with its questions of resolution and S/N. But Adelman et al. (1994) demonstrated that previous claims of photometric variability of  $\alpha$  And based on broadband filter photometry (e.g., Stift 1973) were not confirmed. Their differential Strömgren *uvby* intermediate-band and *Hipparcos* satellite photometry (ESA 1997) both indicate constancy. This is also true of the optical region filter photometry of several nonmagnetic CP stars of the HgMn and metallic-line (Am) classes (Adelman 1993,

1997). Constancy in the optical region imposes stringent limits on photometric variability in the ultraviolet. It refutes the claimed photometric variability of both Rakos (1971) and (Stift 1973), as well as casts considerable doubt on the results of the ultraviolet studies of Rakos & Kamperman (1977) and Rakos, Jenkner, & Wood (1981). A review of the *Hipparcos* photometry of the Am and HgMn stars found some potential intrinsic variables of low amplitude that need to be examined in detail (Adelman 1997), but observations in progress thus far do not find any variability for single stars. As the variable Am stars are mostly eclipsing variables, these HgMn stars might also be such systems.

Zverko, Ziznovsky, & Khokhlova (1997), who used 1.7 Å mm<sup>-1</sup> photographic observations with an instrumental profile half-width of 13 km s<sup>-1</sup> (0.17 Å) and an S/N of 50, claimed that the eclipsing variable HgMn star AR Aur (Nordstrom & Johansen 1994) exhibits variations in the Hg II  $\lambda$ 3984 line. Takeda, Takada, & Kitamura (1979) earlier reached a similar conclusion. But these suggestions require confirmation at higher S/N and resolution with linear detectors.

As for many very bright stars, the literature contains reports of optical region spectroscopic variability for  $\alpha$  And (HR 15, HD 358). For example, Zverko, Hric, & Ziznovsky (1990) using 8.5 Å mm<sup>-1</sup> coude spectrograms claimed rapid variability for the Ca II K line. We obtained 2.4 Å mm<sup>-1</sup> Dominion Astrophysical Observatory (DAO) spectrograms on several nights with a CCD detector and S/N  $\geq$  500 that contained this line. On a given night, the spectra repeated faithfully to within the observational errors, while between nights differences were due to the orbital motion of the secondary relative to the primary. Malanushenko (1996) found

<sup>1</sup> Visiting Observer, Dominion Astrophysical Observatory.

variability of the Si II  $\lambda 6374$  and  $\lambda 6371$  lines with the orbital period due to lines from the secondary, but none for He I  $\lambda 6678$ . He found a period of 1.012344 days for his measurements. Near  $\lambda 6678$  there is a variable line at  $\lambda 6668$  whose width is much less than the wider stellar lines. Another feature near  $\lambda 6683$  appears to behave similarly. As this region contains telluric features, the narrow features are probably telluric, and any periods close to one day reflect the sidereal period.

Ryabchikova, Malanushenko, & Adelman (1999) performed abundance analyses of both components of  $\alpha$  And using data including  $2.4 \text{ \AA mm}^{-1}$  DAO spectrograms obtained with a Reticon detector and  $S/N \geq 200$ . The primary is approximately 2 mag brighter than the secondary in the optical region. Both primary and secondary are broad-lined with  $v_e \sin i$  values of 52 and  $100 \text{ km s}^{-1}$ , respectively. During this study, one of the authors (T. A. R.) noticed that the Hg II  $\lambda 3984$  line profile was peculiar because it did not show the basic rotational line profile. All other spectroscopic changes in any spectral region with more than one exposure and in regions of overlap were explainable in terms of binarity. An examination of the raw data of the spectrogram containing the Hg II  $\lambda 3984$  line did not reveal any problems with the exposure.

The explanation of the mercury isotope anomaly proposed by Michaud, Reeves, & Charland (1974) and the observations of Mègeessier, Michaud, & Weiler (1980) require that mercury be concentrated in a thin layer where the radiative force is just equal to the gravitational forces. More recently, Proffitt et al. (1999) calculated the radiative forces on Hg in the atmospheres of the cool HgMn stars  $\chi$  Lupi and HR 7775. Their observed Hg abundances cannot be supported in these atmospheres by radiative forces alone. They hypothesize that weak mixing can bring Hg into the line-forming region from below the photosphere and that a wind is needed to support a cloud of Hg III at very small optical depths. We are observing a hydrodynamic competition between forces that buoy Hg upward and those that carry it downward. Although we found reasonable agreement with *IUE* observations of  $\alpha$  And for several Hg II and Hg III lines using stratified atmospheres with a Hg enhanced layer near where Hg II is ionized to Hg III to synthesize the observations, as the Hg abundance is also a function of surface position (see below) other important constraints must be included in such calculations to have definitive results.

## 2. OBSERVATIONS

To investigate the anomalous Hg II  $\lambda 3984$  line profile, new observations were made at the DAO coude at a dispersion of  $2.4 \text{ \AA mm}^{-1}$  with a  $15 \text{ \mu m}$  pixel CCD detector centered at  $\lambda 3970$  and a coverage of  $63 \text{ \AA}$ . The FWHM of comparison lines in this configuration is  $0.090 \text{ \AA}$  ( $6.8 \text{ km s}^{-1}$ ). Raw exposures were reduced by a custom program CCDSPEC created by Gulliver & Hill (2002) for optimization of S/N. A wavelength calibration was applied, and spectra were resampled at  $0.036 \text{ \AA}$  intervals. Table 1 is an observing log of our exposures. For the spectra shown in Figure 1, which constitute those that first definitively confirmed the spectrum variability of the Hg II  $\lambda 3984$  line, rectification was performed by matching 12 points in the observed profiles with a synthetic spectrum calculated using the ATLAS9 (Kurucz 1995) and SYNTHE (Kurucz & Avrett 1981) codes with the abundances of Ryabchikova et

TABLE 1  
 $\lambda 3970$  EXPOSURES OF  $\alpha$  ANDROMEDAE

Exposure	Date (UT)	HJD 24,400,000+	S/N	Velocity
W489313659 .....	1993 Oct 19	49,279.6898	570	0.7
W122988496 .....	1998 Jun 21	50,985.8538	210	-24.5
W122989015 .....	1998 Jul 6	51,000.9132	570	-13.8
W1229811353 .....	1998 Jul 30	51,024.8063	530	4.8
W1229811357 .....		51,024.8913	560	4.8
W1229811363 .....		51,024.9667	550	4.8
W1229811561 .....	1998 Aug 2	51,027.9093	390	7.9
W1229811565 .....		51,027.9701	480	7.9
W1229811567 .....		51,027.9909	720	7.9
W1229811664 .....	1998 Aug 3	51,028.8920	590	8.9
W1229811666 .....		51,028.9139	570	8.9
W1229811668 .....		51,028.9382	670	8.9
W1229811670 .....		51,028.9622	670	8.9
W1229811672 .....		51,028.9861	850	8.9
W1229811778 .....	1998 Aug 4	51,029.8830	550	10.0
W1229811780 .....		51,029.9084	610	10.0
W1229811783 .....		51,029.9528	680	10.0
W1229811785 .....		51,029.9751	650	10.0
W1229811787 .....		51,030.0008	580	10.0
W1229816471 .....	1998 Sep 20	51,076.6957	850	-28.1
W1229816476 .....		51,076.7415	580	-28.1
W1229816478 .....		51,076.7793	500	-28.1
W1229816484 .....		51,076.8471	700	-28.0
W1229816485 .....		51,076.8554	540	-28.0
W1229816523 .....		51,076.8880	400	-28.0
W1229816524 .....		51,076.9030	490	-28.0
W1229816525 .....		51,076.9193	700	-28.0
W1229816527 .....		51,076.9415	540	-28.0
W1229816528 .....		51,076.9561	600	-27.9
W1229816529 .....		51,076.9703	560	-27.9
W1229816533 .....		51,077.0210	470	-27.9
W1229816534 .....		51,077.0373	680	-27.9
W1229820065 .....	1998 Oct 27	51,113.6694	460	-1.6
W1229820069 .....		51,113.7392	550	-1.6
W1229820073 .....		51,113.8121	500	-1.6
W1229820080 .....		51,113.9052	325	-1.6
W1229820084 .....		51,114.0017	325	-1.6
W1229820245 .....	1998 Nov 8	51,125.6405	1000	8.9
W1229820253 .....		51,125.7987	1000	9.2
W122999855 .....	1999 Aug 23	51,413.8663	1000	7.0
W122999858 .....		51,413.8795	1000	7.0
W122999860 .....		51,413.8910	900	7.0
W122999862 .....		51,413.9028	1000	7.0
W122999866 .....		51,413.9601	750	7.0
W122999868 .....		51,413.9907	750	7.0
W122999870 .....		51,414.0184	1000	7.0
W1229911691 .....	1999 Sep 18	51,439.8081	1000	-25.0
W1229911693 .....		51,439.8328	900	-25.0
W1229911698 .....		51,439.9203	1000	-25.2
W1229911702 .....		51,439.9807	1000	-25.5
W1229911706 .....		51,440.0220	1000	-25.5
W1229911756 .....	1999 Sep 19	51,440.7866	1000	-29.5
W1229911760 .....		51,440.8439	1000	-29.5
W1229911765 .....		51,440.9206	900	-29.5
W1229911769 .....		51,440.9859	750	-29.5
W1229911835 .....	1999 Sep 20	51,441.9453	1000	-33.3
W1229911837 .....		51,441.9595	1000	-33.3

al. (1999) and with the parameters,  $T_{\text{eff}} = 14,000 \text{ K}$ ,  $\log g = 3.75$ ,  $\xi = 0.0 \text{ km s}^{-1}$ , and  $v_e \sin i = 52 \text{ km s}^{-1}$ . A scattered light correction of 3.5% (Gulliver, Hill, & Adelman 1996) was applied. The S/N values for these exposures were determined from the mean of the 12 continuum points.

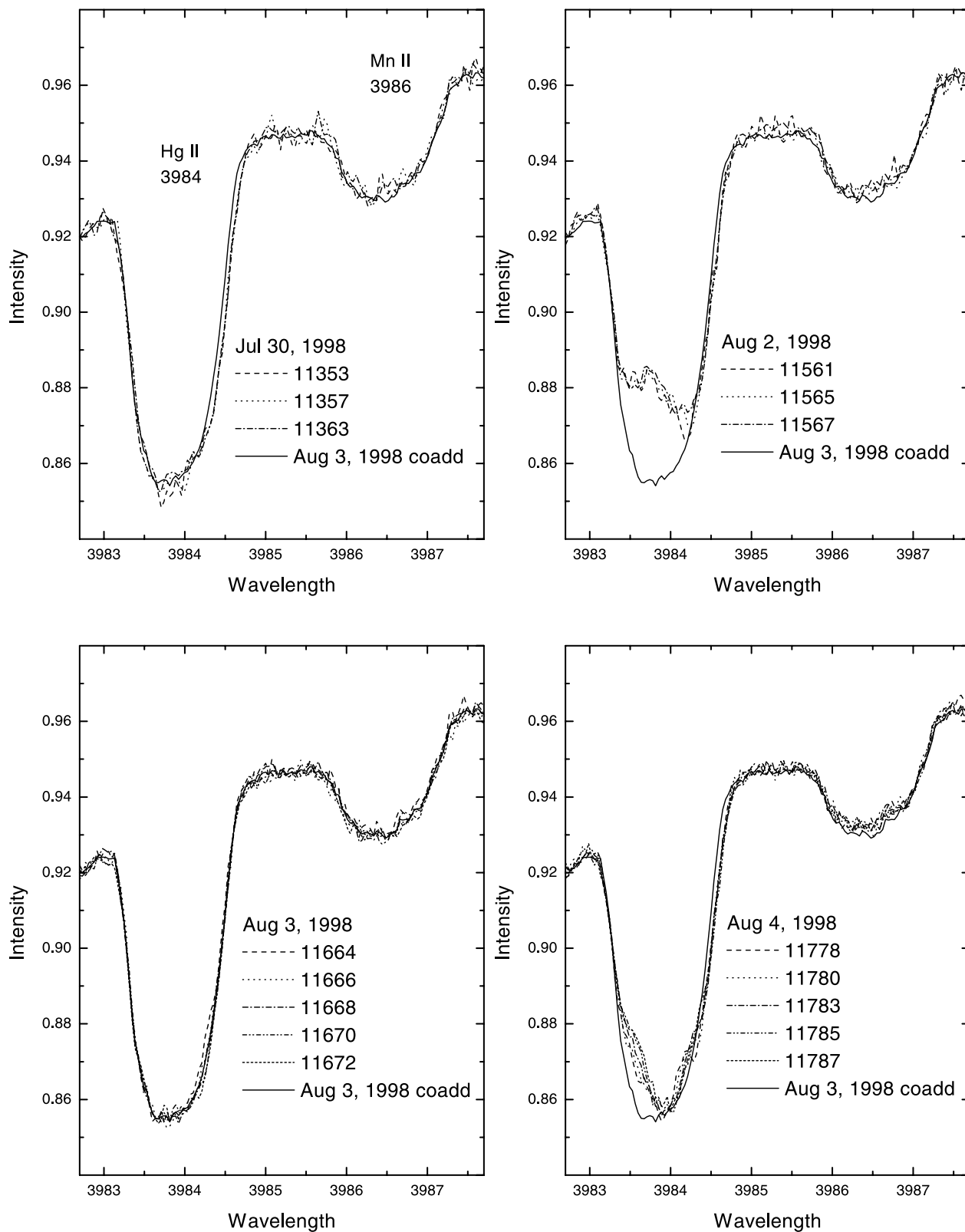


FIG. 1.—Intensity profiles of the Hg II  $\lambda$ 3984 and Mn II  $\lambda$ 3986 lines showing the variation in the former over 6 days. The solid line is the co-added spectrum of 1998 August 3.

### 3. $\alpha$ ANDROMEDAE

The exposures in Figure 1 clearly exhibit different profiles for Hg II  $\lambda$ 3984, but not for the adjacent Mn II  $\lambda$ 3986 line or other observed lines. Figure 2 emphasizes the variations by

ratioing all exposures by the co-added spectra from 1998 August 3, the night showing the least variation. With an orbital period of 96.7015 days (Ryabchikova et al. 1999) the companion's contribution cannot cause these changes as both those in its radial velocity are too small between expo-

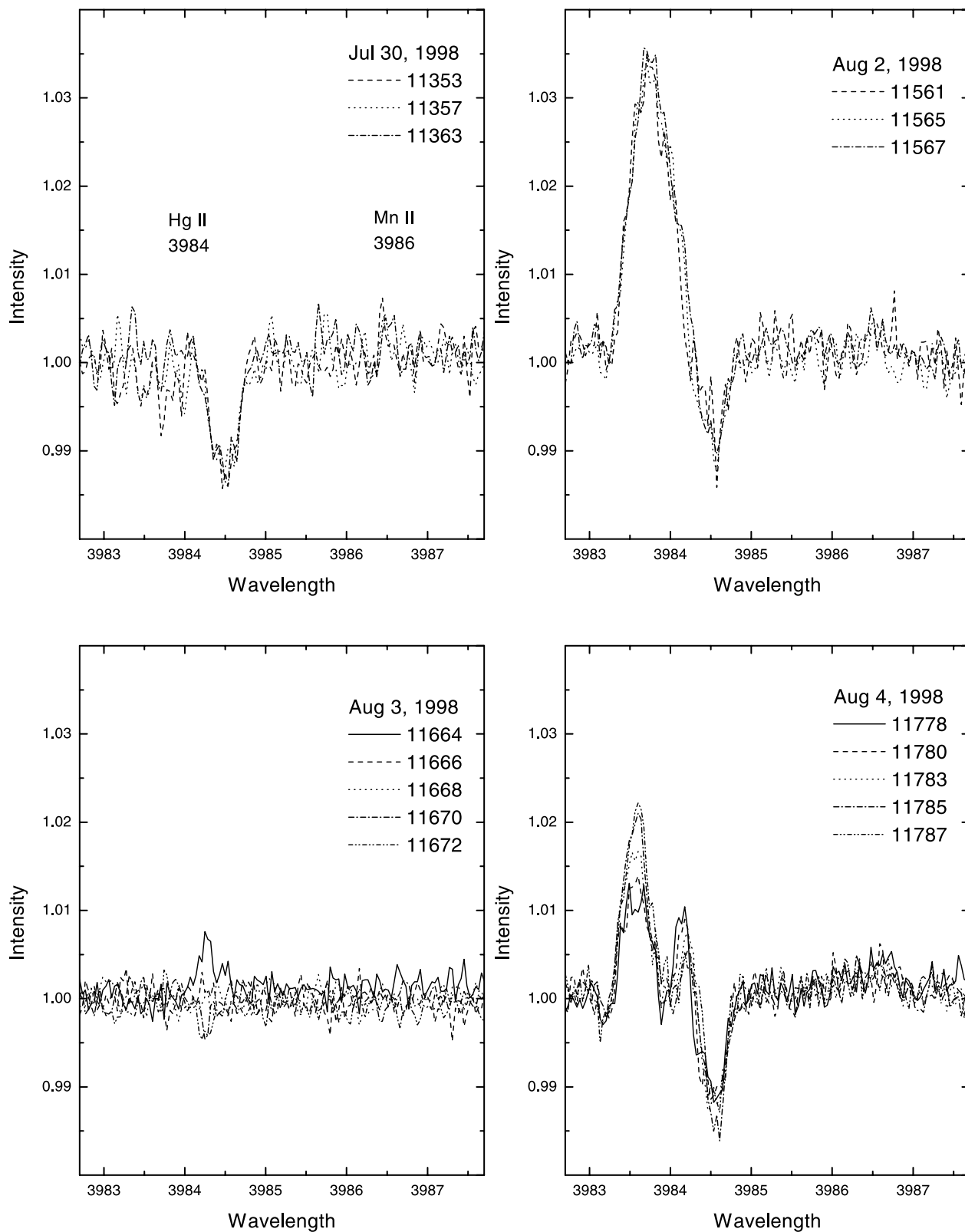


FIG. 2.—Intensity profiles of the Hg II  $\lambda 3984$  and Mn II  $\lambda 3986$  lines, normalized with the co-added spectrum of 1998 August 3

tures during a night and it lacks a  $\lambda 3984$  line. Since the primary produces the lines in Figures 1 and 2, the spectra were shifted to rest velocity using the observed velocities in Table 1, which were determined by cross-correlation of each exposure with the previously described synthetic spectrum over

two  $20 \text{ \AA}$  sections ( $\lambda\lambda 3940\text{--}3960$  and  $\lambda\lambda 3980\text{--}4000$ ). The Hg II  $\lambda 3984$  variations explain the results of Cowley & Aikman (1975), who measured the mean wavelength of Hg II  $\lambda 3984$  on a few  $2.4 \text{ \AA mm}^{-1}$  DAO photographic spectrograms each for several HgMn stars. Their mean wave-

length for  $\alpha$  And was very uncertain as several plates gave values widely discordant from others. With much higher S/N spectrograms we can see the cause for their concern. Inspection of Figures 1 and 2, which contain the profiles from nights in one observing run, shows changes taking place during a given night and more obviously from night to night.

These figures show that intranight variations on time-scales of a few hours are much smaller than the variations from night to night. The largest night to night variation occurred between August 2 and 3. The equivalent widths measured on the co-added spectrum of each night changed by 17%, from 76 to 89 mÅ. The August 3 profile can be fitted well using a standard rotational profile with a  $v_e \sin i = 52 \pm 1 \text{ km s}^{-1}$ . That is not true for the previous night's profiles. Variations are generally largest in the line core with the outer blue wing of the line showing no apparent variation. During a given night, successive spectra show a tendency for minor spectral features to advance to the red, as would be expected if rotation is generating the changes. The magnitude and wavelength extent of the minor spectral features can also apparently change. Nearly the same Hg II  $\lambda$ 3984 line profile was observed on August 2 as on an earlier exposure dated 1993 October 19. Ilyin (2000) confirmed this variability with exposures taken in 1999.

The observed spectrum variability implies that Hg has a nonuniform photospheric distribution. The companion is sufficiently distant and less luminous that it does not cause significant tides or reflection effects. The Hg II  $\lambda$ 3984 line can display isotopic shifts and isotopic broadening. The isotopic wavelengths range from  $\lambda$ 3983.769 for  $^{196}\text{Hg}$  to  $\lambda$ 3984.071 for  $^{204}\text{Hg}$  (Smith 1997). Preston et al. (1971) found that the isotopic shifts correlate with stellar effective temperature. As the primary of  $\alpha$  And has an effective temperature of 13,800 K (Ryabchikova et al. 1999), one would expect a central wavelength of  $\lambda$ 3983.95, comparable to the observed value of  $\lambda$ 3983.90  $\pm$  0.02 found for the rotational profile fitted to the August 3 profile and also close to that for natural (terrestrial) Hg  $\lambda$ 3983.96 (Reader & Corliss 1980).

There are no other sufficiently clean Hg lines in the optical spectrum of  $\alpha$  And, but the ultraviolet has several whose behavior may be similar. An examination of the three short-wavelength primary (SWP) high-dispersion exposures taken by the *IUE* satellite in the region of Hg II  $\lambda$ 1942 shows that the feature has the same profile in the two exposures SWP 14953 and SWP 14954 taken close together on 1981 September 11 and has a profile that is about 10% deeper in SWP 40447 taken on 1990 December 24. This is suggestive of variability. Mégeessier et al. (1980) investigated lines of Hg II and Hg III observed in the *Copernicus* satellite spectrum of  $\alpha$  And; they found absorption features at every wavelength at which a line was expected. To extend this work requires observations using the *Hubble Space Telescope*. Furthermore, such effects have not been observed in other HgMn stars, although this might simply reflect a limited number of high-resolution, high S/N observations and/or a much smaller effect. However, they might be confined to a limited range of effective temperature and are more difficult to observe in sharper lined stars. Rather than being confined to a single star, they are more likely to affect a temperature range of HgMn stars or perhaps the entire class. These issues are amenable to investigation using ground-based coude or echelle spectrographs with modern solid state detectors.

#### 4. PERIOD SEARCH

The mercury line Hg II  $\lambda$ 3984 shows complex variations, which cannot be easily quantified by a single observable, such as equivalent width or line centroid. Thus, we searched for periodicity in the variations of its line profile by studying flux changes in each individual pixel. All observed spectra were interpolated onto a common wavelength grid containing 57 wavelength bins between  $\lambda$ 3983.0 and  $\lambda$ 3984.9. Then we computed separate normalized Lomb periodograms (Press et al. 1992) for each bin. Individual power spectra were subsequently averaged to characterize variability of the whole line profile. Figure 3 shows this average periodogram for the frequency range 0.2–2.2  $\text{day}^{-1}$ . The highest peak in the periodogram is close to 0.42  $\text{day}^{-1}$ . Detailed analysis of the high-resolution power spectrum in this frequency region suggests  $\nu = 0.41987 \pm 0.00069 \text{ day}^{-1}$  or  $P = 2.3817 \pm 0.0039 \text{ days}$  for the main period of the mercury line variations. The probable error was estimated from the width of the corresponding peak in the average power spectrum.

Our standard periodogram analysis is essentially equivalent to a fit with a single harmonic. This model is unlikely to be an adequate approximation of the real variation of the Hg II  $\lambda$ 3984 line profile. If the variation is caused by a complex nonuniform mercury abundance distribution over the  $\alpha$  And A surface, as is likely, then we can hope to improve the period determination by using a more sophisticated parameterization of the line-profile variability, e.g., including higher harmonics in the line-profile fit. To refine the period we used the formula suggested by Schrijvers et al. (1997), who performed a similar time series analysis of the line profile variations of pulsating stars,

$$I_{ij}^{\text{obs}} = I_i^{(0)} + \sum_{k=1}^3 I_i^{(k)} \sin\left(k \frac{T_j - T_0}{P} + \Psi_i^{(k)}\right), \quad (1)$$

where  $I_{ij}^{\text{obs}}$  is the observed flux in the  $i$ th wavelength bin of the  $j$ th normalized spectrum,  $I_i^{(0)}$  is an approximation of the average profile, while  $I_i^{(k)}$  and  $\Psi_i^{(k)}$  are, respectively, the amplitude and phase of the  $k$ th harmonic component. We adopted the heliocentric Julian date of our first observation of  $\alpha$  And A as the reference time  $T_0$ . For each trial period between 2.3778 and 2.3856 days, we adjusted parameters

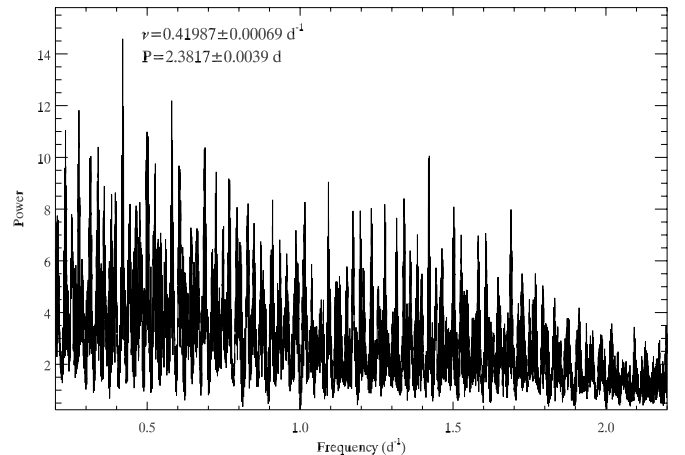


Fig. 3.—Average normalized Lomb periodogram of the variations of the Hg II  $\lambda$ 3984 line reveals the highest peak near 0.42  $\text{day}^{-1}$ .

$I_i^{(0)}$ ,  $I_i^{(k)}$ , and  $\Psi_i^{(k)}$  using the nonlinear least-squares Marquardt optimization method (Bevington & Robinson 1992). A minimum is located at  $P = 2.38236$  days and  $\chi^2_\nu = 2.17$ . An uncertainty (one standard deviation) of this period determination can be estimated by fixing all parameters in equation (1) at their optimal values and finding the deviation from the best-fit period that increases the reduced  $\chi^2$  by unity. This results in  $\sigma_P = 0.00011$  days. The final ephemeris of the Hg II  $\lambda 3984$  variations becomes

$$\text{HJD} = 2449279.6898 + (2.38236 \pm 0.00011)E. \quad (2)$$

Figure 4 confirms that the derived period is fairly consistent with the equivalent width variations of the Hg II  $\lambda 3984$  line. The equivalent width curve is characterized by a broad maximum near phase 0.4 and a narrower minimum at phase 0.0.

All our observations of the mercury line profile, phased together with  $P = 2.38236$  days, are displayed in Figure 5, which also shows a more detailed view of the phase interval 0.8–0.9. The latter interval is particularly densely covered by our spectra and where several observations from the 1998 and 1999 seasons nearly overlap in phase. The comparison of spectra, acquired at similar phases but different observing seasons (e.g., pairs at phases 0.842 and 0.877), shows that the overall shape of the Hg II  $\lambda 3984$  line profile is well reproduced, but some minor discrepancies cannot be excluded. With the data currently available, we are not able to ascribe these apparent changes in the variability pattern to either an error in period determination or slow changes of the mercury distribution on the surface of  $\alpha$  And A.

The rotational period of  $\alpha$  And A can be estimated from the usual relation with the stellar radius  $R$  and inclination of the rotational axis  $i$ :

$$P = \frac{50.613 \sin i R}{v_e \sin i R_\odot}, \quad (3)$$

where the rotational period is measured in days and the rotational velocity  $v_e \sin i$  in kilometers per second. Ryabchikova et al. (1999) found  $v_e \sin i = 52 \pm 2 \text{ km s}^{-1}$  and  $R = 2.7 \pm 0.4 R_\odot$ , while Pan et al. (1992) obtained the

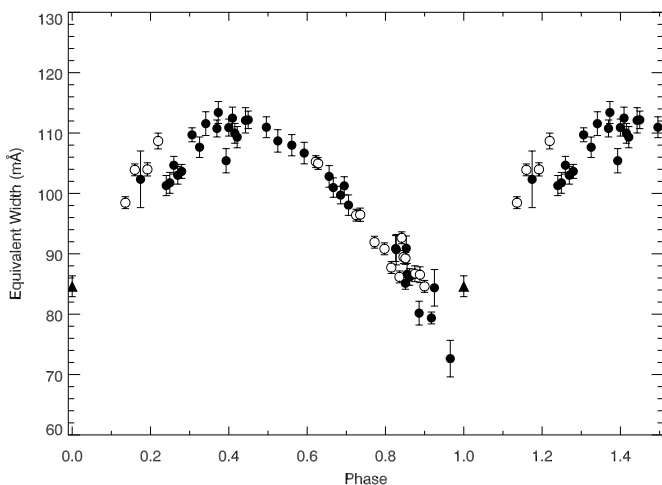


FIG. 4.—Variations of the equivalent width of the Hg II  $\lambda 3984$  spectral line. Observations obtained in 1998 are shown by filled circles and spectra from 1999 by open circles; the filled triangle corresponds to a single spectrum obtained in 1993.

inclination of the binary orbit,  $i_{\text{orb}} = 105^\circ.66 \pm 0^\circ.22$ , from the interferometric measurements. Making the plausible assumption that the rotational axis of  $\alpha$  And A is perpendicular to the plane of the orbital motion,  $i = i_{\text{orb}}$  (or, equivalently,  $i = 180^\circ - i_{\text{orb}}$ ) and, using equation (3), we find  $P = 2.53 \pm 0.39$  days, in good agreement with the period of the Hg II  $\lambda 3984$  line profile variability. This agreement supports the hypothesis that rotational modulation due to surface nonuniformities in the Hg abundance produces the spectral changes that we have discovered for the mercury line. The rotational period of  $\alpha$  And A derived in our paper is also in agreement with the period  $P = 2.38257 \pm 0.00024$  days suggested by Ilyin (2000) on the basis of independent observations of the Hg II  $\lambda 3984$  line.

## 5. DOPPLER IMAGING OF THE Hg ABUNDANCE DISTRIBUTION

Nonuniform chemical abundance distributions exist on the surfaces of the magnetic chemically peculiar stars. These are believed to be produced by chemical diffusion modified by the global magnetic field (e.g., Michaud, Charland, & Mègešsier 1981). However,  $\alpha$  And A is apparently a typical HgMn star, a class for which no reliable detection of a global magnetic field has been achieved.

The brightness of  $\alpha$  And makes it an ideal target for very accurate photopolarimetric magnetic measurements. Borra & Landstreet (1980) and later Glagolevskij et al. (1985) obtained 11 longitudinal field measurements well distributed over the rotation period of the primary star and using, respectively, hydrogen H $\beta$  and metal lines. Neither of these studies achieved a detection of the global magnetic field, placing an upper limit of  $\approx 50$  G on the strength of a global magnetic field. These longitudinal field measurements do not exclude the possibility that fairly strong complex magnetic fields can exist on the surface of  $\alpha$  And A and remain undetected in circular polarization due to the cancellation of contributions from different parts of the stellar surface. However, from a theoretical point of view, it appears quite unlikely that such complex hypothetical magnetic structures can have any physical connection with the fairly simple mercury distribution that we derived with Doppler imaging (see below).

Therefore, we can only speculate that an inhomogeneous mercury distribution on the surface of  $\alpha$  And A was created by diffusion in a weak magnetic field that is still to be detected. However, other time-dependent hydrodynamic effects that alter the diffusion process cannot be excluded. The first possibility could imply a relatively stable surface abundance map that would change only on timescales comparable to the stellar lifetime (Mègešsier 1984), while the second possibility might lead to short-term variability of the Hg surface map and, consequently, to a detectable change in the variability pattern of the Hg II  $\lambda 3984$  spectral line. We hope to distinguish between these two scenarios by monitoring variability of the mercury line for several years and constructing independent Doppler maps for each of the observing seasons. As the best phase coverage was obtained for the 1998 season, we used a subset of our 37 spectra of  $\alpha$  And obtained in 1998 to construct the first map of the abundance nonuniformities on the surface of a HgMn star.

Doppler Imaging (DI) is a complex technique that can reconstruct features on the surfaces of stars by inverting a time series of high-resolution spectral line profiles into a

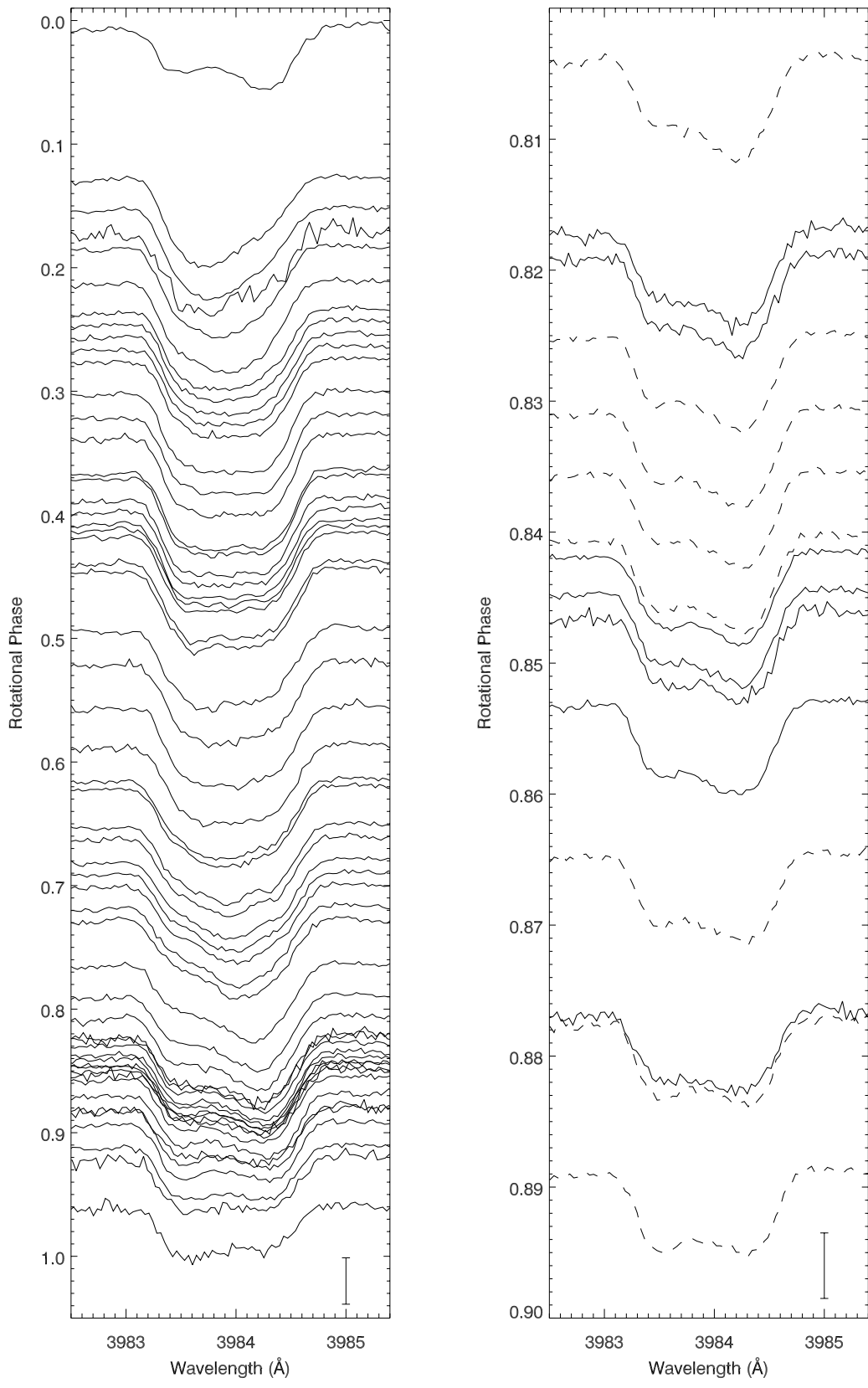


FIG. 5.—*Left*: All profiles of the Hg II  $\lambda 3984$  spectral line phased together using a period of 2.38236 days. Spectra for the consecutive phases are shifted in the vertical direction. *Right*: A more detailed view of our data in the phase interval 0.8–0.9. In this panel spectra obtained during the 1998 season are shown by the solid lines, while dashed lines correspond to the observations from the 1999 season. The vertical scale is indicated by the bars at the lower right of each panel. The bars correspond to 10% of the continuum flux.

map of the stellar surface. The basic concepts of DI have been reviewed in several papers, which described the application of this technique to the imaging of specific local parameters of the stellar photospheres. This includes temperature mapping of the late-type active stars (Vogt, Penrod, & Hatzes 1987; Rice & Strassmeier 2000), reconstruction of the abundance distributions on the surfaces of chemically peculiar stars (Rice, Wehlau, & Khoklova 1989), and imaging of the magnetic field on the active late-type stars (Brown et al. 1991). For the reconstruction of the mercury abundance map we used the DI code INVERS12, which allows simultaneous imaging of several chemical elements using spectroscopic data from multiple wavelength intervals. Kuschnig et al. (1999) used an early version of this code for the abundance mapping of the chemically peculiar stars.

Prior to performing the DI analysis, the spectra of  $\alpha$  And A must be corrected for the effects related to the binary nature of this star. First, we shifted the wavelength scale of all our observations to the reference frame of the primary star using the orbital solution of Ryabchikova et al. (1999). In addition, we corrected the dilution of the  $\alpha$  And A spectrum by the continuum radiation of the secondary star using their stellar parameters and radii ratio ( $R_a/R_b = 1.64$ ). Their model atmosphere of  $\alpha$  And A was also used in our DI analysis. An inclination angle of  $i = 74^\circ$  was adopted for the abundance mapping as outlined in the previous section.

The mercury line is in the red wing of the hydrogen H $\epsilon$  line, which results in a small reduction of the residual depth of the Hg II  $\lambda 3984$  line. We normalized our high-resolution  $\alpha$  And spectra relative to a pseudocontinuum of the H $\epsilon$  wing but explicitly accounted for the blending by the hydrogen line in the calculations of the synthetic spectra by adding hydrogen bound-bound transitions to the continuous opacity sources.

The line list used for the DI consisted of 15 isotopic and hyperfine components of the Hg II  $\lambda 3984$  line and a Y II  $\lambda 3982.594$  line blending with the blue wing of the mercury feature. The wavelengths and relative strengths of the isotopic and hyperfine components of Hg II  $\lambda 3984$  are from Woolf & Lambert (1999), while the total oscillator strength  $\log(gf) = -1.529$  is from Proffitt et al. (1999). The parameters of the Y II transition were extracted from the VALD database (Kupka et al. 1999).

Because of the rapid rotation of  $\alpha$  And A, the isotope components of the Hg II  $\lambda 3984$  line are not resolved. In principle, INVERS12 allows us to treat each of the stable Hg isotopes as a separate abundance distribution and to reconstruct six abundance maps from a single blend. However, our observational data are insufficient for such an approach, and recovery of the individual maps for each of the Hg isotopes based on only one spectral line would not be reliable. Hence, we parameterized the mercury isotope composition using the isotopic-fractionation model of White et al. (1976). With this formalism the relative abundance of each of the Hg isotopes is given by a simple function of a single parameter  $q$  (see Smith 1997, eqs. [1]–[3]), which describes the deviation of the stellar Hg isotope mixture from the terrestrial isotope composition. Large values of the  $q$ -parameter imply an isotope mixture biased toward the heaviest Hg isotopes, while  $q = 0$  corresponds to the terrestrial isotope composition. A change in the  $q$ -parameter is essentially equivalent to a change of the mean wavelength of the Hg II transition. We modified our

DI code to allow mercury abundance mapping using a fixed isotope composition or the simultaneous recovery of both the total Hg abundance and the surface distribution of the  $q$ -parameter.

Recent studies of sharp-lined HgMn stars featuring resolved isotopic components of Hg II  $\lambda 3984$  showed that the isotopic mixture in some stars cannot be fitted with the  $q$ -parameter formalism (Woolf & Lambert 1999; Hubrig, Castelli, & Mathys 1999). However, using the  $q$ -parameter (or some equivalent simple parameterization) is probably the only meaningful way of studying possible deviations of the Hg isotopic composition from the solar mixture in stars like  $\alpha$  And, in which the isotopic splitting of this mercury lines is completely smeared out by the rotational broadening.

We refined the value of the projected rotational velocity of  $\alpha$  And A and determined the average Hg isotope composition by carrying out multiple Doppler reconstructions for a set of  $v_e \sin i$  and  $q$ -parameter values. The best fit to the observed profiles was achieved for  $v_e \sin i = 52 \pm 1 \text{ km s}^{-1}$  and  $q = -0.25 \pm 0.15$ . This projected rotational velocity coincides with the  $v_e \sin i$  obtained by Ryabchikova et al. (1999), while the value of the  $q$ -parameter indicates that the average Hg isotope composition in  $\alpha$  And A departs only slightly from the terrestrial mixture and is shifted in favor of the lighter Hg isotopes.

The results of the DI recovery of the mercury abundance distribution using the isotope composition fixed at its optimal value are presented in Figure 6, with a spherical map in Figure 8a. The mercury overabundance is strongly concentrated toward the equatorial region of the star, where the average Hg abundance reaches  $\log(N_{\text{Hg}}/N_{\text{tot}}) \approx -5.0$ . In addition to the equatorial belt of enhanced Hg abundance, we found three small areas of extreme Hg overabundance located on the rotational equator at longitudes  $l = 90^\circ$ ,  $170^\circ$ , and  $270^\circ$ , with values as high as  $\log(N_{\text{Hg}}/N_{\text{tot}}) \approx -3.0$ . At the same time, Hg abundances on the stellar surface at latitudes greater than  $\pm 30^\circ$  are typically  $\log(N_{\text{Hg}}/N_{\text{tot}}) \approx -7.5$ .

We also tested the hypothesis of a nonuniform mercury isotope composition. Figures 7b and 8c show the results of the simultaneous recovery of the  $q$ -parameter and Hg abundance maps. In comparison with the Doppler reconstruction using a fixed value of the  $q$ -parameter, the Hg map recovered when allowing for surface variations of the isotope composition shows a slight decrease of the contrast of the mercury abundance map and a somewhat improved fit to the observed line profiles (the average deviation for the mapping with a fixed  $q$ -parameter was 0.317%, while the DI code achieved an average deviation of 0.297% when both the abundance and the isotope composition of Hg were imaged). The  $q$ -parameter map suggests that a concentration of heavy Hg isotopes may exist in two surface regions located at the equator and longitudes  $l = 120^\circ$  and  $l = 180^\circ$ – $260^\circ$ . However, given the relatively low amplitude of the changes of the  $q$ -parameter over the surface of  $\alpha$  And A and the very small difference between synthetic spectra computed with and without surface variations in the isotope composition, we conclude that even if surface variations in the Hg isotope mixture are real, they do not have a pronounced impact on the variability of the Hg II  $\lambda 3984$  line. Additional very high S/N observations of this and other mercury lines are needed to confirm that Hg abundance spots on the surface of  $\alpha$  And A are indeed accompanied by surface variability of the mercury isotope mixture.

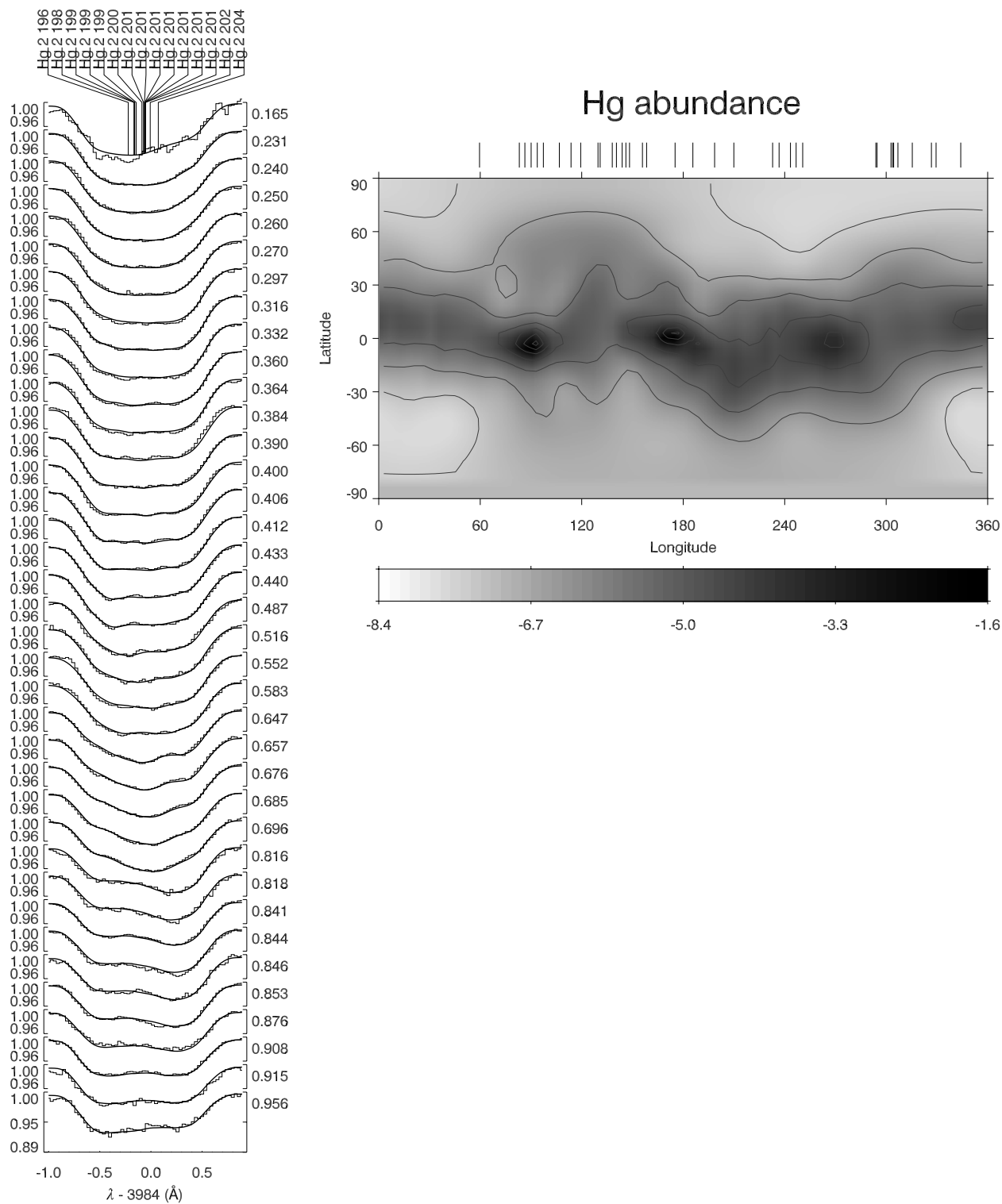


FIG. 6.—Results of the DI reconstruction of the mercury surface distribution using a fixed Hg isotope mixture ( $q = -0.25$ ). The column to the left compares observed (*histograms*) and computed (*solid curves*) profiles of the Hg II  $\lambda 3984$  line. The spectra for the consecutive rotational phases are shifted in the vertical direction. The rectangular plot shows a pseudo-Mercator projection of the Hg surface map. The solid curves shown on top of the gray-scale image are contours of equal abundance, plotted for  $\log(N_{\text{Hg}}/N_{\text{tot}})$  values between  $-8$  and  $-2$  with a 1 dex step. The tick marks above the map visualize the phase coverage of the spectra employed in our Doppler mapping.

6. CONCLUSIONS

The discovery of the spectrum variability of the Hg II  $\lambda 3984$  line provides both observational and theoretical challenges. Finding a set of analogues may not be easy since

definitive observations of this line profile and its variability requires spectra with both high resolution and signal-to-noise ratio. Such objects will certainly not be as bright, nor the geometry as likely to be so favorable as to reveal the Hg variability.

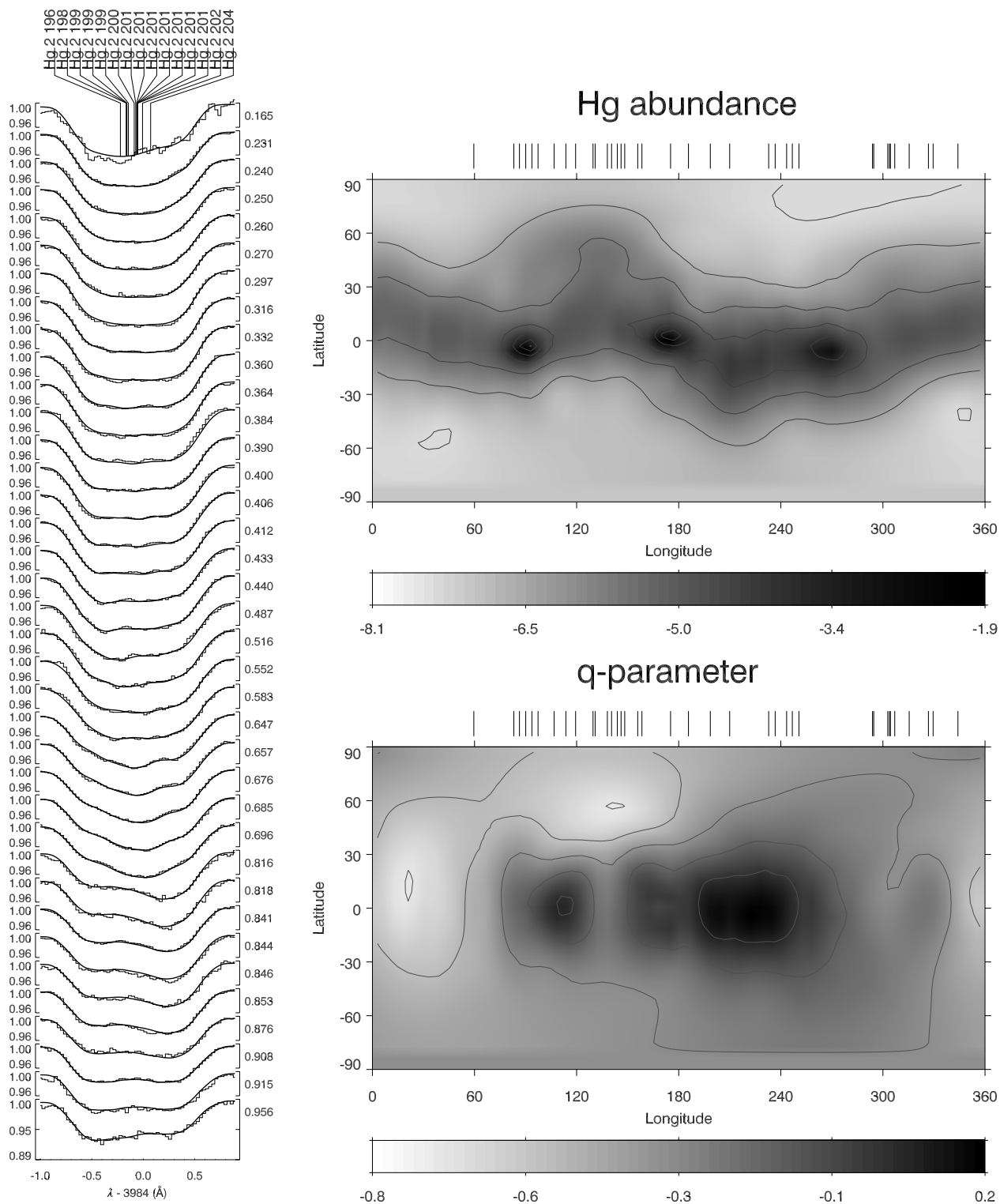


FIG. 7.—Same as in Fig. 6, but for the simultaneous DI of the Hg abundance and isotope composition parameterized by the  $q$ -parameter

Hubrig & Mathys (1995) suggest from the study of HgMn stars in binary systems that Hg is preferentially distributed along their rotational equators, while Mn is strongly concentrated near their poles. The very sharp lined HgMn star 53 Tau A, which lacks a Hg  $\Pi$   $\lambda$  3984 line, is thus seen with a rotational pole toward the Earth. But the analysis of  $\alpha$  And A by Ryabchikova et al. (1999) and the spectra examined in this study show that the apparent rotational velocities of

Mn  $\Pi$  lines are consistent with the rotational velocities obtained from features other than Hg  $\Pi$   $\lambda$  3984, and hence Mn is unlikely to be strongly concentrated around the poles. Furthermore, there are other sharp-lined HgMn stars in binary systems such as  $\iota$  CrB that have strong Hg  $\Pi$   $\lambda$  3984 lines. It is more likely that the variability shown by  $\alpha$  And A is confined to a narrow range of stellar parameters rather than characterizing the entire class of HgMn stars.

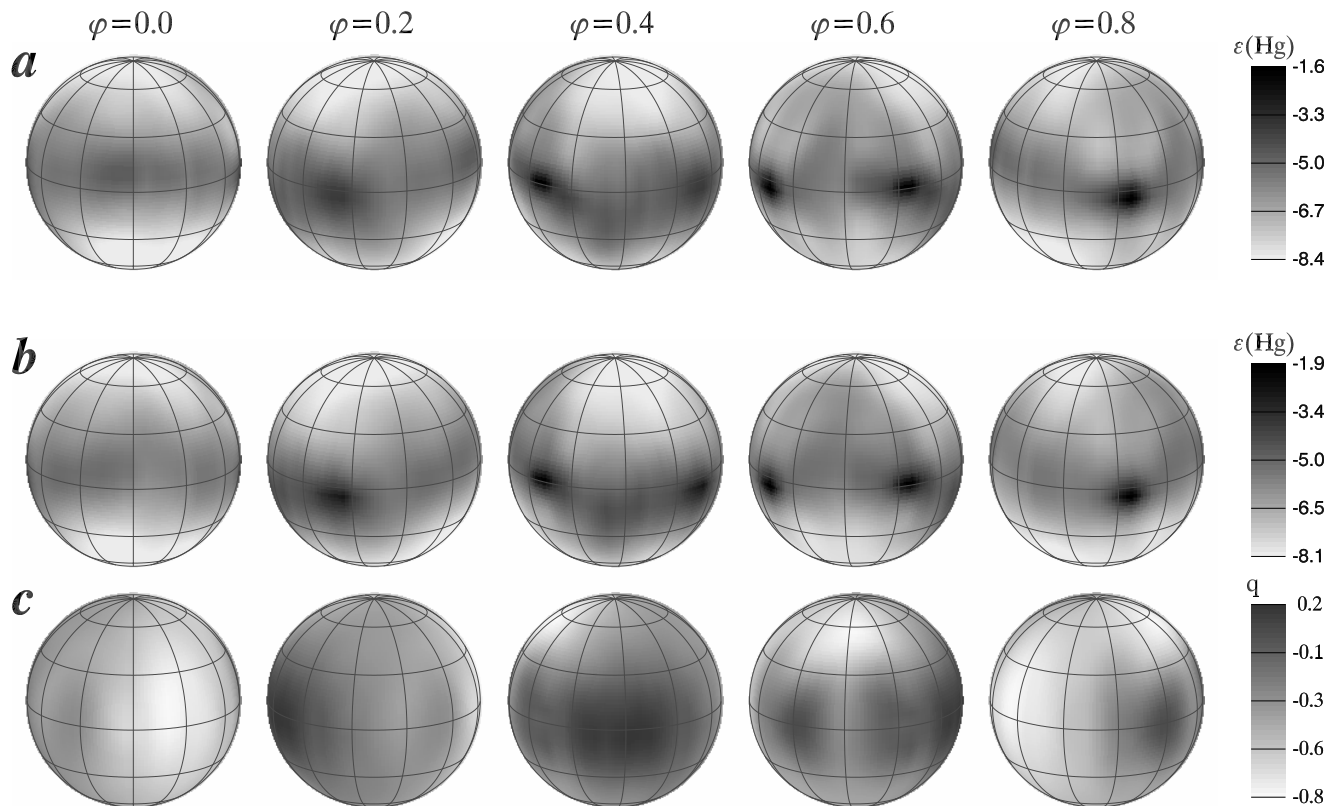


FIG. 8.—Spherical DI maps of the star shown at five equidistant rotational phases, viewed at the inclination angle  $i = 74^\circ$ , for (a) the Hg abundance for a fixed  $q = -0.25$ , (b) the Hg abundance for the simultaneous DI with variable abundance and isotopic composition, and (c) the  $q$  parameter as for (b).

For  $\alpha$  And, variability in other Hg II and Hg III lines is expected, but separating their contributions from blends could be problematic for weaker lines. Are their conditions of formation sufficiently different to provide new sets of modeling constraints? Theoretically, one must explain why Hg is concentrated in a nonuniform equatorial band. Perhaps one might invoke a magnetic field. Clearly some physics must distinguish the behavior of the polar and equatorial regions. Furthermore, the question of long-term stability of the equatorial band on both a global and localized basis must be investigated.

This work was supported in part by grants from The Citadel Foundation to S. J. A. Financial support was provided to A. F. G. by the National Sciences and Engineering Research Council of Canada. S. J. A. and A. F. G. appreciate the help of their service observer Frank Younger in obtaining some of these spectrograms. T. A. R. thanks the Fonds zur Förderung der wissenschaftlichen Forschung (project P-14984), the Russian National Program “Astronomy,” and RFBR (grant 00-15-96722) for partial funding.

#### REFERENCES

- Adelman, S. J. 1993, *A&A*, 269, 411  
 ———. 1997, *A&AS*, 123, 445  
 Adelman, S. J., Brown, B. H., Caliskan, H., Reese, D. F., & Adelman, C. J. 1994, *A&AS*, 106, 333  
 Bevington, P. R., & Robinson, D. K. 1992, *Data Reduction and Error Analysis for the Physical Sciences* (2d ed.; New York: McGraw-Hill)  
 Borra, E. F., & Landstreet, J. D. 1980, *ApJS*, 42, 421  
 Brown, S. F., Donati, J.-F., Rees, D. E., & Semel, M. 1991, *A&A*, 250, 463  
 Cowley, C. R., & Aikman, G. C. L. 1975, *PASP*, 87, 513  
 European Space Agency. 1997, *The Hipparcos and Tycho Catalogs*, ed. M. A. C. Perryman (ESA SP-1200; Noordwijk: ESA)  
 Glagolevskij, Yu. V., Romanyuk, I. I., Bychkov, V. D., & Najdenov, I. D. 1985, *Soviet Astron. Lett.*, 11, 45  
 Gulliver, A. F. & Hill, G. 2002, *PASP*, in press  
 Gulliver, A. F., Hill, G., & Adelman, S. J. 1996, in *ASP Conf. Ser. 108, Model Atmospheres and Spectrum Synthesis*, ed. S. J. Adelman, 7F. Kupka, & W. W. Weiss (San Francisco: ASP), 232  
 Hubrig, S., Castelli, F., & Mathys, G. 1999, *A&A*, 341, 190  
 Hubrig, S., & Mathys, G. 1995, in *ASP Conf. Ser. 81, Laboratory and Astronomical High Resolution Spectra*, ed. A. J. Sauval, A. Blomme, & N. Grevesse (San Francisco: ASP), 555  
 Ilyin, I. V. 2000, Ph.D. thesis, Univ. Oulu, Finland  
 Kupka, F., Piskunov, N., Ryabchikova, T. A., Stempels, H. C., & Weiss, W. W. 1999, *A&AS*, 138, 119  
 Kurucz, R. L. 1995, in *ASP Conf. Ser. 78, Astrophysical Applications of Powerful New Databases*, ed. S. J. Adelman & W. L. Wiese (San Francisco: ASP), 205  
 Kurucz, R. L., & Avrett, E. H. 1981, *SAO Special Rep.* 391  
 Kuschnig, R., Ryabchikova, T. A., Piskunov, N. E., Weiss, W. W., & Gelbmann, M. J. 1999, *A&A*, 348, 924  
 Leckrone, D. S., Wahlgren, G. M., & Johansson, S. 1991, *ApJ*, 377, L37  
 Malanushenko, V. P. 1996, *Astrophysics*, 39, 208  
 Mègeessier, C. 1984, *A&A*, 138, 267  
 Mègeessier, C., Michaud, G., & Weiler, E. J. 1980, *ApJ*, 239, 237  
 Michaud, G. 1970, *ApJ*, 160, 641  
 Michaud, G., Charland, Y., & Mègeessier, C. 1981, *A&A*, 103, 244  
 Michaud, G., Reeves, H., & Charland, Y. 1974, *A&A*, 37, 313  
 Nordstrom, B., & Johansen, K. T. 1994, *A&A*, 282, 787  
 Pan, X., et al. 1992, *ApJ*, 384, 624  
 Press, W. H., Teukolsky, S. A., Vetterling, W. T., & Flannery, B. P. 1992, *Numerical Recipes* (2d ed.; Cambridge: Cambridge Univ. Press)  
 Preston, G. W., Vaughan, A. H., White, R. E., & Swings, J. P. 1971, *PASP*, 83, 607  
 Proffitt, C. R., Brage, T., Leckrone, D. S., Wahlgren, G. M., Brandt, J. C., Sansonetti, C. J., Reader, J., & Johansson, S. G. 1999, *ApJ*, 512, 942  
 Rakos, K. D. 1971, *IAU Colloq. 15, New Directions and New Frontiers in Variable Star Research* (Bamberg: Remeis-Sternwarte), 599  
 Rakos, K. D., Jenkner, H., & Wood, J. 1981, *A&AS*, 43, 209

- Rakos, K. D., & Kamperman, T. M. 1977, *A&A*, 55, 53  
Reader, J., & Corliss, C. H. 1980, *Wavelengths and Transition Probabilities for Atoms and Atomic Ions, Part I* (Washington: GPO)  
Rice, J. B., & Strassmeier, K. G. 2000, *A&AS*, 147, 151  
Rice, J. B., Wehlau, W. H., & Khokhlova, V. L. 1989, *A&A*, 208, 179  
Roby, S. R., Leckrone, D. S., & Adelman, S. J. 1999, *ApJ*, 524, 974  
Ryabchikova, T. A., Malanushenko, V. S., & Adelman, S. J. 1999, *A&A*, 351, 963  
Schrijvers, C., Telting, J. H., Aerts, C., Ruymaekers, E., & Henrichs, H. F. 1997, *A&AS*, 121, 343  
Seaton, M. J. 1996, *Phys. Scr.*, 65, 129  
———, 1999, *MNRAS*, 307, 1008  
Smith, K. C. 1997, *A&A*, 319, 928  
Stift, M. J. 1973, *A&A*, 22, 209  
Takeda, Y., Takada, M., & Kitamura, M. 1979, *PASJ*, 31, 821  
Vogt, S. S., Penrod, G. D., & Hatzes, A. P. 1987, *ApJ*, 321, 496  
Wahlgren, G. M., Leckrone, D. S., Johansson, S. G., Rosberg, M., & Brage, T. 1995, *ApJ*, 444, 438  
White, R. E., Vaughan, A. H., Preston, G. W., & Swings, J. P. 1976, *ApJ*, 204, 131  
Woolf, V. M., & Lambert, D. L. 1999, *ApJ*, 521, 414  
Zverko, J., Hric, L., & Ziznovsky, J. 1990, *Contrib. Astron. Obs. Skalnaté Pleso*, 20, 143  
Zverko, J., Ziznovsky, J., & Khokhlova, V. L. 1997, *Contrib. Astron. Obs. Skalnaté Pleso*, 27, 41